Kataoka and Ngwira *Progress in Earth and Planetary Science* (2016) 3:23
DOI 10.1186/s40645-016-0101-x

Progress in Earth and
Planetary Science

REVIEW

Open Access

Extreme geomagnetically induced currents

Ryuho Kataoka[1,2*] and Chigomezyo Ngwira[3,4]

Abstract

We propose an emergency alert framework for geomagnetically induced currents (GICs), based on the empirically extreme values and theoretical upper limits of the solar wind parameters and of d*B*/d*t*, the time derivative of magnetic field variations at ground. We expect this framework to be useful for preparing against extreme events. Our analysis is based on a review of various papers, including those presented during Extreme Space Weather Workshops held in Japan in 2011, 2012, 2013, and 2014. Large-amplitude d*B*/d*t* values are the major cause of hazards associated with three different types of GICs: (1) slow d*B*/d*t* with ring current evolution (RC-type), (2) fast d*B*/d*t* associated with auroral electrojet activity (AE-type), and (3) transient d*B*/d*t* of sudden commencements (SC-type). We set "caution," "warning," and "emergency" alert levels during the main phase of superstorms with the peak Dst index of less than −300 nT (once per 10 years), −600 nT (once per 60 years), or −900 nT (once per 100 years), respectively. The extreme d*B*/d*t* values of the AE-type GICs are 2000, 4000, and 6000 nT/min at caution, warning, and emergency levels, respectively. For the SC-type GICs, a "transient alert" is also proposed for d*B*/d*t* values of 40 nT/s at low latitudes and 110 nT/s at high latitudes, especially when the solar energetic particle flux is unusually high.

Keywords: Geomagnetically induced currents, Magnetic storms, Auroral substorms, Sudden commencements, Solar energetic particles

Review

Geomagnetically induced currents (GICs) are an important natural space weather hazard for our global modern society which depends on power grids (Royal Academy of Engineering Report 2013; Tsurutani et al. 2015). The motivation of this paper is to contribute to the 2015 NASA Living with a Star Institute GIC Working Group, where we aimed to understand the basic properties of extreme GICs for a robust operation of power grids to mitigate the potential hazard from extreme GIC events.

To predict large-amplitude GICs, the most essential parameter is d*B*/d*t*, the time derivative of the local magnetic field at ground. Detailed time-frequency representations of d*B*/d*t* during intense magnetic storms have been investigated (e.g., Pulkkinen and Kataoka 2006; Kataoka and Pulkkinen 2008; Pulkkinen et al. 2010; Tsurutani and Lakhina 2014). GIC events with large-amplitude d*B*/d*t* values can be categorized into three different types: (1) magnetic storms or ring current evolution characterized by slow d*B*/d*t* values globally with a timescale of hours (RC-type); (2) substorm activities in which aurora electrojet currents cause fast d*B*/d*t* in auroral regions with a timescale of several minutes (AE-type); and (3) sudden commencements in which rapid compression of the magnetosphere causes global enhancement of d*B*/d*t* with a timescale of tens of seconds (SC-type).

Here, on the basis of a review of extreme events and important recent papers, we propose an emergency alert framework that takes into account the different timescales and largest observed amplitudes of RC-type, AE-type, and SC-type GICs.

RC-type slow GICs

The emergency level of GICs can be well defined by the magnetic storm level because large-amplitude, global, and long-duration GICs are associated with the evolution of the ring current on a timescale of 10–60 min. It is also worth noting here that, depending on ground conductivities, slow GICs can also be the most effective source of GICs at low magnetic latitudes, for example, in Hokkaido, Japan (Watari et al. 2009; Pulkkinen et al. 2010).

The "Halloween storms" of 29–31 October 2003 threatened electrical grids in South Africa and Sweden (Pulkkinen et al. 2005). This double-peaked superstorm reached minimum Dst index values of −353 and −383 nT on 29 and 30

---

* Correspondence: kataoka.ryuho@nipr.ac.jp
[1]National Institute of Polar Research, Tokyo, Japan
[2]Department of Polar Science, SOKENDAI, Tokyo, Japan
Full list of author information is available at the end of the article

October, respectively (Mannucci et al. 2005). The maximum dB/dt amplitude as estimated from the Dst index was 100 nT/h. The largest magnetic storm on record during the space age (the last half century), which occurred on 13 March 1989 (Allen et al. 1989), led to the collapse of the Hydro-Quebec high-voltage power transmission system (Bolduc 2002). The peak Dst index was −589 nT, and the maximum dB/dt amplitude was 130 nT/h. The SYM-H value (the symmetric disturbance index for the H-component, 1 min time cadence) for this storm was −710 nT (Lakhina and Tsurutani 2016). The occurrence rate of a storm comparable to the March 1989 storm has been estimated to be once every 60 years (Tsubouchi and Omura 2007; Riley 2012; Kataoka 2013), although it has been argued that such storms cannot be predicted with reasonable accuracy (Willis et al. 1997; Tsurutani et al. 2003; Love 2012; Yermolaev et al. 2013; Love et al. 2015; Lakhina and Tsurutani 2016). The solar wind parameters were not very extreme at the time of the 1989 storm. For example, Nagatsuma et al. (2015) estimated that the solar wind speed of 960 km/s and southward interplanetary magnetic field Bz of −50 nT continuing for 5 h drove the main phase of the March 1989 storm, whereas Lakhina and Tsurutani (2016) indicated that the interplanetary driver of the March 1989 storm included multiple shocks, multiple sheaths, and multiple magnetic clouds. It is therefore reasonable to assume that a perfect "slot machine"-type combination of solar wind parameters sometimes results from the complex interactions of chains of coronal mass ejections during their propagation in the solar wind (Cid et al. 2014; Kataoka et al. 2015).

The largest magnetic storm in magnetometer history (last 170 years), the "Carrington storm," occurred on 2 September 1859 and was observed at Colaba (magnetic latitude = 9.6°) in Bombay (Tsurutani et al. 2003). The peak Dst index has been estimated as −1760 nT (Tsurutani et al. 2003), −850 nT (Siscoe et al. 2006), and −900 nT (Cliver and Dietrich 2013). Its dB/dt amplitude was therefore 6.0×10^2 nT/h on average because the main phase duration was 1.5 h. Another "Carrington-like" storm (with a comparable amplitude of -825 nT $<$ Dst $<$ -900 nT), which occurred on 15 May 1921 at Apia, Samoa (−15.3°), had a dB/dt amplitude of 3.0×10^2 nT/h (Angenheister and Westland 1921; Silverman and Cliver 2001). Both the Carrington storm and the May 1921 storm caused disruptions of telegraph services (Boteler 2006). The occurrence rate of a storm comparable to the Carrington storm is about once per century (Love et al. 2015). It is worth noting that a rapid recovery phase of a superstorm can also cause a high dB/dt amplitude in a slow RC-type GIC (Keika et al. 2015).

To prepare for unprecedented extreme storms, larger than the Carrington storm, theoretical discussions can help us to understand the upper limits of the Dst index and of dB/dt for the "emergency" alert level. Vasyliunas (2011) suggested that the upper limit of the Dst index is -2.5×10^3 nT. The estimated time to reach the saturation value during the development of such a superstorm is 2–6 h (Vasyliunas 2013). The dB/dt amplitude would therefore range from 4.0×10^2 to 1.25×10^3 nT/h. In fact, a naive estimation from solar wind parameters, in particular the largest in situ observed values of the interplanetary magnetic field B (=1.0×10^2 nT; Russell et al. 2013) and solar wind speed V (=2240 km/s; Skoug et al. 2004), made by extending the empirical relationship reported by O'Brien and McPherron (2000), gives a maximum injection rate of ring current energy of 9.8×10^2 nT/h. Note that Tsurutani and Lakhina (2014) estimated the maximum possible interplanetary magnetic field and solar wind speed to be 127 nT and 2700 km/s, respectively.

Recorded superstorms are listed in Table 1. In our emergency alert framework, we set the criterion for the first alert level, "caution," to Dst $<$ −300 nT for a slow GIC (10–60 min) timescale, with an expected dB/dt of around 100–150 nT/h. All such slow GIC effects are global, and their duration is several hours, that is, the typical duration of the main phase of magnetic storms. The "warning" level is assigned to superstorms somewhat larger than the March 1989 storm (Dst $<$ −600 nT), which have an expected dB/dt in the range of 150–400 nT/h. The "emergency" alert is for superstorms as large as or larger than the Carrington storm (Dst $<$ −900 nT) with an expected dB/dt of 400–1250 nT/h.

AE-type fast GICs

The largest dB/dt variations are associated with substorm activities at high magnetic latitudes, although these substorm effects can extend even to middle and low magnetic latitudes during extreme events. The record largest rapid change in the north-south component dH recorded at middle latitudes was 1710 nT at Greenwich (53.3°) on 25 September 1909 (Cliver and Svalgaard 2004). On the same day, dH $>$ 1500 nT was observed at Potsdam, Germany (52.6°) (Tsurutani et al. 2003). A telegraph interruption that occurred at Tokyo (magnetic latitude = 25.3°) on 25 September 1909 was the first Japanese accidental example of GICs (Uchida 1909). The magnetometer record at Tokyo was off-scale (H-component maximum = −200 nT), but the initial rapid decrease of 200 nT occurred within 5 min at around 1140 UT, that is, at the onset, the dB/dt amplitude was >40 nT/min, a result that is hard to interpret without considering substorm activities. Local midnight at Tokyo is at 1500 UT,

Table 1 Historical hazardous RC-type GIC events

Date	−Dst (nT)	d*B*/d*t* (nT/h)	Note
2 September 1859	850[a] (900[b])	600	Historically largest storm
15 May 1921	825–900[b]	>400	Low-latitude auroras[c]
13, 14 March 1989	589	130	Largest storm in the space age since 1957
29, 30 October 2003	353, 389	100	GIC hazardous superstorms

[a] Siscoe et al. (2006)
[b] Cliver and Dietrich (2013)
[c] Silverman and Cliver (2001)

and an aurora was seen that night at Sapporo (32.7° magnetic latitude) and at Niigata (27.5° magnetic latitude).

Akasofu and Kamide (2005) proposed that the "H-spike" of the 1859 Carrington storm was due to field-aligned currents, but Tsurutani et al. (2005) rejected that proposal. More recently, Cliver and Dietrich (2013) reported that the H-spike recorded at Colaba (9.6°) during the Carrington storm included contributions from aurora-related currents, because of the similarity between the Colaba magnetometer time series and that of the May 1847 storm recorded at Greenwich (53.3°). The most notable observation of activity was made at Rome (38.8°), where Secchi (1859) reported a decrease of -3.0×10^3 nT in the H-component. Similar levels of perturbation (3.5×10^3 nT) at middle latitudes for a Carrington-type superstorm event were simulated in a study by Ngwira et al. (2014). More recently, on the basis of a comparison of the Halloween storms and the Carrington storm, Cid et al. (2015) hypothesized that the auroral current system can influence the middle to low latitudes during superstorms, especially in the pre-noon sector. The mechanism of this pre-noon enhancement is straightforward: Not only ionospheric currents but also upward field-aligned currents induce a negative north-south (H-component) excursion at middle to low latitudes in the pre-noon sector during superstorms. In fact, Tsuji et al. (2012) reported that d*H* enhancement was highly localized in the magnetic local time direction during the main phase of a storm in the middle latitudes (35–55°), possibly owing to the d*H* contribution from upward field-aligned currents. We note, however, that Lakhina and Tsurutani (2016) recently presented a rebuttal of the hypothesis of Cid et al. (2015).

If the importance of field-aligned currents is assumed, then such aurora-related effects cannot be negligible in the middle to low latitudes. The local area of influence of an AE-type GIC with large-amplitude d*B*/d*t* can extend to a latitude 20° lower than the equatorward boundary of the auroral oval, even though the d*B*/d*t* amplitude is only an order of magnitude smaller than its amplitude in the high latitudes (Ngwira et al. 2013, 2014). By extending the empirical relationship of Yokoyama et al. (1998), the equatorward boundary of the auroral oval during the Carrington storm can be extrapolated down to 30° magnetic latitude (peak Dst = −900 nT), whereas during most superstorms with peak Dst < −300 nT, the boundary is at 36–43° magnetic latitude. More studies are needed to investigate how such an extreme equatorward boundary of the auroral oval can occur because recent simulations have pointed to a saturation level of aurora oval expansion (Ngwira et al. 2013), although there are contemporary reports of a low-latitude aurora during the Carrington event (Kimball 1960). One of the most equatorward auroras ever reported was observed during the Carrington event. Kimball (1960) has pointed out that red auroras were detected at ±23°, and Tsurutani et al. (2003) estimated the Dst index of the Carrington event by assuming that the plasmapause during the storm was located at ±23°. The largest known auroral extent was observed at 19° magnetic latitude on 4 February 1872 (Cliver and Svalgaard 2004).

For practical purposes, it is worth noting here that the lowest latitude aurora sighting is also 20° lower than the latitude of sightings of the overhead coronal aurora (i.e., of the apparent auroral oval) during extreme events (Silverman and Cliver 2001). Reports of an aurora sighting are therefore a sign of the area of influence of AE-type fast GICs where the d*B*/d*t* amplitude is expected to be an order of magnitude smaller than its high-latitude amplitude.

Viljanen et al. (2014) reported that a d*B*/d*t* as high as 1200 nT/min has been observed at the middle latitude Nurmijärvi station in Finland (56.9°) during superstorms (Dst < −300 nT) such as the Halloween storms and the 13 July 1982 storm (peak Dst = −325 nT). Nakamura et al. (2015) showed statistically that the AU and AL indices have upper limits that give an upper limit of the AE index of 6.0×10^3 nT. In extreme cases, the fast AE-type d*B*/d*t* of 6.0×10^3 nT/min can therefore be observed at high latitudes. The upper limit of the AE index observed so far is 4.4×10^3 nT. For example, Tsurutani et al. (2015) reported several super-substorms with an AE index of < −2500 nT and noted that the AE index of the largest event reached −4418 nT.

In our emergency alert framework, the "caution" level poses the maximum d*B*/d*t* of 2.0×10^3 nT/min at magnetic latitudes >40° during the main phase of superstorms

Table 2 Historical hazardous events with SC-type transient GICs

Date	Record	Notes
24 March 1940	$\mathrm{d}H > 273$ nT at KAK[a]	Second largest storm ($\mathrm{d}H = -661$ nT) at KAK
13 November 1960	$\mathrm{d}H = 220$ nT at KAK[a]	GLE10[b], 3rd largest 30 MeV SEP[c]
4 August 1972	Shortest transit time, GIC[d]	GLE24[f], 8th largest 30 MeV SEP[c]
24 March 1991	$\mathrm{d}H = 202$ nT[f], GIC[g]	Largest 10 MeV SEP[h]

[a] Magnetometer observations at Kakioka (Araki 2014)
[b] Steljes et al. (1961)
[c] Cliver and Svalgaard (2004)
[d] Lanzerotti (1983)
[e] http://neutronm.bartol.udel.edu/~pyle/GLE_List.txt (GLE stands for the ground level enhancement of neutron monitor counting rate caused by the most energetic SEP)
[f] Araki (1997)
[g] Kappenman (2003)
[h] http://umbra.nascom.nasa.gov/SEP/

with Dst < −300 nT. At lower latitudes, the largest possible local GIC effect is expected to be a $\mathrm{d}B/\mathrm{d}t$ of 2.0×10^2 nT/min. The “warning” level poses the maximum $\mathrm{d}B/\mathrm{d}t$ of 4.0×10^3 nT/min at middle to high latitudes during the main phase of storms with Dst < −600 nT. During these storms, a local GIC effect of $\mathrm{d}B/\mathrm{d}t = 4.0 \times 10^2$ nT/min is expected at low latitudes. For extreme, stronger-than-Carrington storms (Dst < −900 nT), the “emergency” level poses the maximum $\mathrm{d}B/\mathrm{d}t$ level of 6.0×10^3 nT/min at middle to high latitudes, and at low latitudes, the largest possible local GIC effect is expected to be $\mathrm{d}B/\mathrm{d}t = 6.0 \times 10^2$ nT/min.

SC-type transient GICs

Sudden commencements (SCs) cause global, large-amplitude, transient GICs, especially in the high-frequency domain. For example, the 24 March 1991 SC event had a peak $\mathrm{d}B/\mathrm{d}t$ of 40 nT/s for tens of seconds at low latitudes (Kappenman 2003). One of the largest known SCs occurred on 24 March 1991 at Kakioka (26.6°) around the noon sector (Araki et al. 1997). The northward magnetic field change $\mathrm{d}H$ rapidly increased up to 202 nT within 1.0 min. Recently, Araki (2014) reported two historically large SCs were recorded at Kakioka on 13 November 1960 ($\mathrm{d}H = 220$ nT) and on 24 March 1940 ($\mathrm{d}H > 273$ nT). Another historically large SC ($\mathrm{d}H = 308$ nT) was recorded only at Alibag (10.3°) on 7 July 1928. Because at the same time $\mathrm{d}H$ was only 8 nT at Kakioka, this particular July 1928 event tells us that local enhancement of an SC can occur in the low latitudes. Interestingly, almost all large SC events have been clustered in the maximum and early declining phase of sunspot cycles (Araki 2014).

The $\mathrm{d}B/\mathrm{d}t$ amplitudes of SC-type GICs basically depend on the dynamic pressure of the solar wind. This solar wind parameter dependence is essentially different from the parameter dependence of $\mathrm{d}B/\mathrm{d}t$ amplitudes of RC-type and AE-type GICs, which mainly depend on the southward component of the interplanetary magnetic field and the solar wind speed. A “transient alert” of SC-type GICs is always in effect when caution, warning, or emergency alerts are issued, because during such superstorm situations incoming interacting chains of fast coronal mass ejections are likely, and rapid variations of the solar wind dynamic pressure can always occur. In addition to during superstorms, however, a “transient alert” should be issued whenever the flux of solar energetic particles (SEPs), which is accelerated by fast coronal mass ejections, is unusually high. In fact, extremely high speed solar wind events and super SC events are always accompanied by very high SEP flux events or superstorms (Table 2).

The complex waveform of the largest SCs can be interpreted by examining the so-called DL and DP components (Araki et al. 1997), where DL denotes a step-like disturbance dominant at low latitudes (global compression), and DP denotes an impulsive disturbance of polar origin (current vortices associated with a preliminary impulse and a main impulse). The timescale of the DL component can be derived from the shock transit time over an effective length of 30 Earth radii (Araki et al. 2004), and the timescale of the DP component can be derived from the shock transit time over an effective length of 3.5 Earth radii (Kubota et al. 2015). The shortest transit time on record, from the flare onset to the shock arrival at the Earth, of 14.6 h occurred on 4 August 1972 (Vaisberg and Zastenker 1976) for an average propagation speed

Table 3 Parameters for the GIC emergency alert model. The criterion for each alert level is shown in the second column, and the following columns show the expected extreme $\mathrm{d}B/\mathrm{d}t$ values for RC-, AE-, and SC-type GICs

		$\mathrm{d}B/\mathrm{d}t$ of GICs		
Alert level	Criterion	RC (nT/h)	AE (nT/min)	SC (nT/s)
Caution	Dst < −300 nT	100–150	2000	40–110
Warning	Dst < −600 nT	150–400	4000	40–110
Emergency	Dst < −900 nT	400–1250	6000	40–110
Transient alert	High SEP flux			40–110

of 2850 km/s (Tsurutani and Lakhina 2014), which is faster than the second shortest transit time of 17.5 h during the Carrington event. A similarly short transit time of 15–17 h from the Sun to the Earth was also reported for the 23 July 2012 STEREO-A event (Russell et al. 2013). If a high shock speed of 2.5×10^3 km/s is assumed, then the DL and DP components would have shortest minimum durations of 76 and 9 s, respectively.

The amplitude of the DL component is proportional to the square root of dynamic pressure (Siscoe et al. 1968), and the extreme DL jump is 320 nT, assuming a dynamic pressure of 460 nPa (Araki 2014). The amplitude of the DP component is also proportional to the square root of dynamic pressure, and the extreme DP is 1.0×10^3 nT at high latitudes and 3.5×10^2 nT at low latitudes (Kubota et al. 2015).

By combining the above extreme values, transient $\mathrm{d}B/\mathrm{d}t$ values for SC-type GICs of 1.1×10^2 nT/s at high latitudes and of 39 nT/s at low latitudes are obtained. In a recent analysis, Fiori et al. (2014) reported data that support these estimates. Note, however, that Tsurutani and Lakhina (2014) estimated a maximum SC-type $\mathrm{d}B/\mathrm{d}t = 30$ nT/s on a 22 s timescale, from a different point of view. The boundary between the two $\mathrm{d}B/\mathrm{d}t$ regimes at high latitudes and at low latitudes changes with the extent of the auroral oval, and we can use the same equatorward boundary of the auroral oval used for "caution/warning/emergency" alerts for the boundary between the two regimes.

Emergency alert framework

In summary, we determined extreme $\mathrm{d}B/\mathrm{d}t$ values for three different types of GICs, slow RC-type, fast AE-type, and transient SC-type GICs. For RC-type and AE-type GICs, we set "caution," "warning," and "emergency" alert levels for magnetic storms with a peak Dst index of less than −300, −600, and −900 nT, respectively. The occurrence rates of storms at the caution, warning, and emergency levels are once every 10, 60 , and 100 years, respectively. The extreme $\mathrm{d}B/\mathrm{d}t$ values of AE-type GICs range from 2000 to 6000 nT/min. For SC-type GICs, a "transient alert" is used for the extreme $\mathrm{d}B/\mathrm{d}t$ values of 110 nT/s at high latitudes and 40 nT/s at low latitudes. The alert criteria and the extreme values are listed in Table 3 and also shown graphically in Fig. 1.

The Dst index, as provided at the website of Kyoto University, must be monitored in real time to use the emergency alert framework. Real-time monitoring of energetic protons of >10 MeV, as observed by the GOES satellites, is also necessary to activate the "transient alert."

Conclusions

The proposed emergency alert framework provides a basic starting point for understanding the expected extreme values of $\mathrm{d}B/\mathrm{d}t$ around the world. Empirical, theoretical, and statistical approaches could improve this framework and make it more detailed. To make the "emergency alert" approach more flexible and dynamic by using physics-based quantitative predictions, a complete parameter survey of both global magnetohydrodynamic and ring current

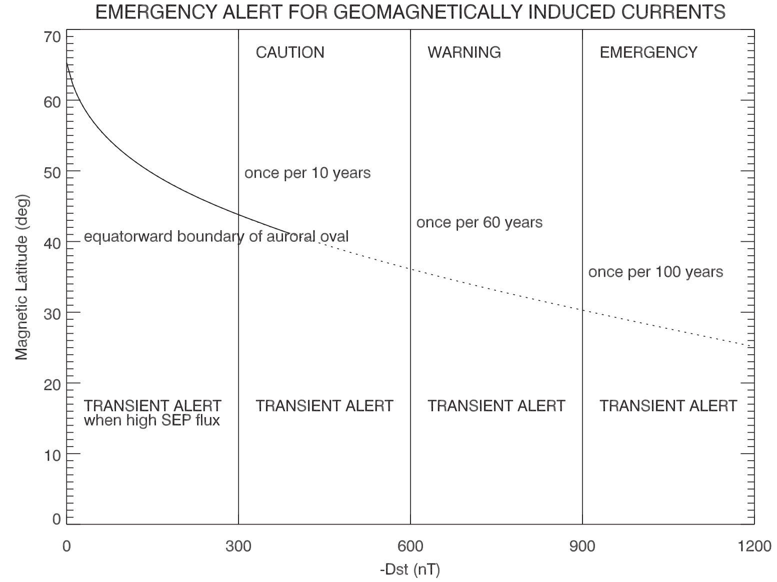

Fig. 1 Emergency alert framework for geomagnetically induced currents. The equatorward boundary of the auroral oval according to the model of Yokoyama et al. (1998) is shown by the *solid curve*, and the *dotted curve* shows its theoretical extrapolation. It is important to update the possible extension of the auroral oval toward middle to low latitudes during extreme magnetic storms

simulations should be performed with various sets of solar wind parameters, such as the interplanetary magnetic field and the solar wind speed and density, to identify the largest dB/dt values of RC-type, AE-type, and SC-type GICs at high, middle, and low latitudes.

Competing interests

The authors declare that they have no competing interests.

Authors' contributions

RK drafted the manuscript. CN advised on the interpretation and helped to draft the manuscript. Both authors read and approved the final manuscript.

Acknowledgements

RK thanks Antti Pulkkinen for helpful discussions. This collaborative study was supported by the NASA Living with a Star Institute GIC Working Group in 2015. The Extreme Space Weather Workshops 2011, 2012, 2013, and 2014 were supported by the Research Institute for Sustainable Humanosphere, Kyoto University; the Solar-Terrestrial Environmental Laboratory, Nagoya University; and the National Institute of Polar Research, Japan.

Author details

[1]National Institute of Polar Research, Tokyo, Japan. [2]Department of Polar Science, SOKENDAI, Tokyo, Japan. [3]Department of Physics, Catholic University of America, Washington, District of Columbia, USA. [4]Space Weather Laboratory, NASA Goddard Space Flight Center, Greenbelt, Maryland, USA.

Received: 6 February 2016 Accepted: 4 August 2016

References

Akasofu S-I, Kamide Y (2005) Comment on "the extreme magnetic storm of 1-2 September 1859" by B. T. Tsurutani, W.D. Gonzalez, G. S. Lakhina, and S. Alex. J Geophys Res 110(10.1029/2005JA011005):A09226

Allen J, Frank L, Sauer H, Reiff P (1989) Effects of the March 1989 solar activity. Eos 70(46):1479, 1486-1488

Angenheister G, Westland CJ (1921) The magnetic storm of May 13-14, 1921: observations at Samoa Observatory. N Z J Sci Technol 4:201–202

Araki T (2014) Historically largest geomagnetic sudden commencement (SC) since 1868. Earth, Planet and Space 66:164

Araki T, Fujitani S, Emoto M, Yumoto K, Shiokawa K, Ichinose T, Luehr H, Orr D, Milling DK, Singer H, Rostoker G, Tsunomura S, Yamada Y, Liu CF (1997) Anomalous sudden commencement on March 24, 1991. J Geophys Res 102(A7):14075–14086. doi:10.1029/96JA03637

Araki T, Takeuchi T, Araki Y (2004) Rise time of geomagnetic sudden commencements—statistical analysis of ground geomagnetic data. Earth, Planets and Space 56:289–293

Bolduc L (2002) GIC observations and studies in the Hydro-Quebec power system. J Atmos Sol Terr Phys 64(16):1793–1802

Boteler DH (2006) The super storms of August/September 1859 and their effects on the telegraph system. Adv Space Res 38:159–172

Cid C, Palacios J, Saiz E, Guerrero A, Cerrato Y (2014) On extreme geomagnetic storms. J Space Weather Space Clim 4:A28. doi:10.1051/swsc/2014026

Cid C, Saiz E, Guerrero A, Palacios J, Cerrato Y (2015) A Carrington-like geomagnetic storm observed in the 21st century. J Space Weather Space Clim 5:A16. doi:10.1051/swsc/2015017

Cliver EW, Dietrich WF (2013) The 1859 space weather event revisited: limits of extreme activity. J Space Weather Space Clim 3:A31. doi:10.1051/swsc/2013053

Cliver EW, Svalgaard L (2004) The 1859 solar-terrestrial disturbance and the current limits of extreme space weather activity. Sol Phys 224:407–422

Fiori RAD, Boteler DH, Gillies DM (2014) Assessment of GIC risk due to geomagnetic sudden commencements and identification of the current systems responsible. Space Weather 12:76–91. doi:10.1002/2013SW000967

Kappenman JG (2003) Storm sudden commencement events and the associated geomagnetically induced current risks to ground-based systems at low-latitude and midlatitude locations. Space Weather 1(3):1016. doi:10.1029/2003SW000009

Kataoka R (2013) Probability of occurrence of extreme magnetic storms. Space Weather 11:1–5. doi:10.1002/swe.20044

Kataoka R, Pulkkinen A (2008) Geomagnetically induced currents during intense storms driven by coronal mass ejections and corotating interacting regions. J Geophys Res 133:A03S12. doi:10.1029/2007JA012487

Kataoka, R., D. Shiota, E. Kilpua, and K. Keika (2015), Pileup accident hypothesis of magnetic storm on 17 March 2015, Geophys. Res. Lett., 42, doi:10.1002/2015GL064816.

Keika K, Ebihara Y, Kataoka R (2015) What caused the rapid recovery of the Carrington storm? Earth, Planets and Space 67:65. doi:10.1186/s40623-015-0234-y

Kimball DS (1960) A study of the aurora of 1859, Sci. Rpt. 6, UAG-R109. Univ. Alaska, Fairbanks, Alaska

Kubota Y, Kataoka R, Den M, Tanaka T, Nagatsuma T, Fujita S (2015) Global MHD simulation of magnetospheric response of preliminary impulse to large and sudden enhancement of the solar wind dynamic pressure. Earth, Planets and Space 67:94. doi:10.1186/s40623-015-0270-7

Lakhina GS, Tsurutani BT (2016) Geomagnetic storms: historical perspective to modern view. Geosci Lett 3:5. doi:10.1186/s40562-016-0037-4

Lanzerotti LJ (1983) Geomagnetic induction effects in ground-based systems. Space Sci Rev 34:347–356

Love JJ (2012) Credible occurrence probabilities for extreme geophysical events: earthquakes, volcanic eruptions, magnetic storms. Geophys Res Lett 39: L10301. doi:10.1029/2012GL051431

Love, J. L., E. J. Rigler, A. Pulkkinen, and P. Riley (2015), On the lognormality of historical magnetic storm intensity statistics: implications for extreme-event probabilities, Geophys. Res. Lett., 42, doi:10.1002/2015GL064842.

Mannucci AJ, Tsurutani BT, Iijima BA, Komjathy A, Saito A, Gonzalez WD, Guarnieri FL, Kozyra JU, Skoug R (2005) Dayside global ionospheric response to the major interplanetary events of October 29-30, 2003 "Halloween storms". Geophys Res Lett 32:L12S02. doi:10.1029/2004GL021467

Nagatsuma T, Kataoka R, Kunitake M (2015) Estimating the solar wind conditions during an extreme geomagnetic storm: a case study of the event that occurred on March 13-14, 1989. Earth, Planets and Space 67:78. doi:10.1186/s40623-015-0249-4

Nakamura M, Yoneda A, Oda M, Tsubouchi K (2015) Statistical analysis of extreme auroral electrojet indices. Earth, Planets and Space 67:153. doi:10.1186/s40623-015-0321-0

Ngwira CM, Pulkkinen A, Wilder FD, Crowley G (2013) Extended study of extreme geoelectric field event scenarios for geomagnetically induced current applications. Space Weather 11:121–131. doi:10.1002/swe.20021

Ngwira CM, Pulkkinen A, Kuznetsova MM, Glocer A (2014) Modeling extreme Carrington-type space weather events using three-dimensional MHD code simulations. J Geophys Res 119:4456–4474. doi:10.1002/2013JA019661

O'Brien TP, McPherron RL (2000) An empirical phase space analysis of ring current dynamics: Solar wind control of injection and decay. J Geophys Res 105(A4):7707–7719

Pulkkinen A, Kataoka R (2006) S-transform view of geomagnetically induced currents during geomagnetic superstorms. Geophys Res Lett 33:L12108. doi:10.1029/2006GL025822

Pulkkinen A, Lindahl S, Viljanen A, Pirjola R (2005) Geomagnetic storm of 29 – 31 October 2003: Geomagnetically induced currents and their relation to problems in the Swedish high-voltage power transmission system. Space Weather 3:S08C03. doi:10.1029/2004SW000123

Pulkkinen A, Kataoka R, Watari S, Ichiki M (2010) Modeling geomagnetically induced currents in Hokkaido, Japan. Adv Space Res 46(9):1087–1093. doi:10.1016/j.asr.2010.05.024

Riley P (2012) On the probability of occurrence of extreme space weather events. Space Weather 10:S02012. doi:10.1029/2011SW000734

Royal Academy of Engineering Report (2013), Extreme space weather impacts on engineered systems and infrastructure, Royal Acad. Eng., Prince Philip House, 3 Carlton House Terr., London SW1Y5DG, UK.

Russell CT et al (2013) The very unusual interplanetary coronal mass ejection of 2012 July 23: a blast wave mediated by solar energetic particles. Astrophysical J 770:38. doi:10.1088/0004-637X/770/1/38

Secchi RP (1859) Sur les perturbations magnetiques observes a Rome le septembre 1859. Comptes Rendus 49:458–460

Silverman SM, Cliver EW (2001) Low-latitude auroras: the magnetic storm of 14-15 May 1921. J Atmos Sol-Terr Phys 63:523–535

Siscoe GL, Formisano V, Lazarus AL (1968) Relation between geomagnetic sudden impulses and solar wind dynamic pressure changes—an experimental investigation. J Geophys Res 73(15):4869–4874

Siscoe G, Crooker NU, Clauer CR (2006) *Dst* of the Carrington storm of 1859. Adv Space Res 38:173–179

Skoug RM, Gosling JT, Steinberg JT, McComas DJ, Smith CW, Ness NF, Hu Q, Burlaga LF (2004) Extremely high speed solar wind: 29?30 October 2003. J Geophys Res 109:A09102. doi:10.1029/2004JA010494
Steljes JF, Carmichael H, McCracken KG (1961) Characteristics and fine structure of the large cosmic-ray fluctuations in November 1960. J Geophys Res 66:5
Tsubouchi K, Omura Y (2007) Long-term occurrence probabilities of intense geomagnetic storm events. Space Weather 5:S12003. doi:10.1029/2007SW000329
Tsuji Y, Shinbori A, Kikuchi T, Nagatsuma T (2012) Magnetic latitude and local time distributions of ionospheric currents during a geomagnetic storm. J Geophys Res 117:A07318. doi:10.1029/2012JA017566
Tsurutani BT, Lakhina GS (2014) An extreme coronal mass ejection and consequences for the magnetosphere and Earth. Geophys Res Lett 41:287–292. doi:10.1002/2013GL058825
Tsurutani BT, Gonzalez WD, Lakhina GS, Alex S (2003) The extreme magnetic storm of 1-2 September 1859. J Geophys Res 108(A7):1268. doi:10.1029/2002JA009504
Tsurutani BT, Gonzalez WD, Lakhina GS, Alex S (2005) Reply to comment by S.-I. Akasofu and Y. Kamide on “the extreme magnetic storm of 1-2 September 1859”. J Geophys Res 110:A09227. doi:10.1029/2005JA011121
Tsurutani BT, Hajra R, Echer E, Gjerloev JW (2015) Extremely intense (SML < -2500 nT) substorms: isolated events that are externally triggered? AnGeo Comm 33:519–524. doi:10.5194/angeocom-33-519-2015
Uchida T (1909) Geomagnetically induced currents on September 25, 1909, J Inst Electrical Engineers Japan, pp 701-721.
Vaisberg OL, Zastenker GN (1976) Solar wind and magnetosheath observations at Earth during August 1972. Space Sci Rev 19:687–702
Vasyliunas VM (2011) The largest imaginable magnetic storm. J Atmos Sol-Terr Phys 73:1444–1446
Vasyliunas VM (2013) Time scale of the largest imaginable magnetic storm, Nonlin. Processes Geophys 20:19–23. doi:10.5194/npg-20-19-2013
Viljanen A, Myllys M, Nevanlinna H (2014) Russian geomagnetic recordings in 1850-1862 compared to modern observations. J Space Weather Space Clim 4:A11. doi:10.1051/swsc/2014008
Watari S, Kunitake M, Kitamura K, Hori T, Kikuchi T, Shiokawa K, Nishitani N, Kataoka R, Kamide Y, Aso T, Watanabe Y, Tsuneta Y (2009) Measurement of geomagnetically induced currents in a power grid in Hokkaido, Japan. Space Weather 7:S03002. doi:10.1029/2008SW000417
Willis DM, Stevens PR and Crothers SR (1997) Statistics of the largest geomagnetic storms per solar cycle (1844–1993). Ann Geophys 15:719–728.
Yermolaev YI, Lodkina IG, Nikolaeva NS, Yermolaev MY (2013) Occurrence rate of extreme magnetic storms. J Geophys Res Space Physics 118:4760–4765. doi:10.1002/jgra.50467
Yokoyama N, Kamide Y, Miyaoka H (1998) The size of the auroral belt during magnetic storms. Ann Geophys 16:566–573